EPSC Abstracts
Vol. 11, EPSC2017-821, 2017
European Planetary Science Congress 2017
© Author(s) 2017

Water ice in Juling crater on Ceres surface: method for properties retrieval

A. Raponi[1], M.C. De Sanctis[1], M. Ciarniello[1], E. Ammannito[2,1], A. Frigeri[1], J.-Ph. Combe[3], F. Tosi[1], F. Zambon[1], F.G. Carrozzo[1], G. Magni[1], M.T. Capria[1], M. Formisano[1], A. Longobardo[1], E. Palomba[1], C.M. Pieters[4], C.T. Russell[5], C.A. Raymond[6], and the Dawn/VIR Team
[1]INAF-IAPS Istituto di Astrofisica e Planetologia Spaziali, Rome, Italy (andrea.raponi@iaps.inaf.it), [2]Agenzia Spaziale Italiana, Rome, Italy. [3]Bear Fight Institute, Winthrop, WA, USA. [4]Department of Earth, Environmental and Planetary Sciences, Brown University, Providence, RI, USA. [5]University of California at Los Angeles, Los Angeles, CA, USA. [6]NASA/Jet Propulsion Laboratory and California Institute of Technology, Pasadena, CA, USA.

Abstract

Spectral signatures diagnostic of water ice were detected in localized areas on the surface of Ceres usingthe Dawn/VIR instrument [1] of the Dawn spacecraft. The current study analyzed water ice detected in a shadowed region of Juling crater. Water ice properties were derived by a Hapke radiative transfer model [2].

1. Introduction

The NASA Dawn spacecraft in orbit around Ceres has been acquiring a huge amount of data at different spatial resolutions during the several phases of the mission that started in 2015. The Visible and InfraRed (VIR) mapping spectrometer [1] onboard Dawn, enabled detection and mapping of the main mineralogical phases on Ceres.
The surface of Ceres is mainly characterized by a large abundance of dark component, NH_4-phillosilicates and carbonates [3]. Other mineralogical phases, such as water ice, also exist at local scale [4, 5] . Water ice detected in Juling crater (lon=168°, lat=35°S) is not under direct solar illumination. However, it is visible becouse of secondary illumination coming from the crater floors and rims. A specific modeling is required to derive water ice properties such as abundance, grain size, phase, type of mixture with the average dark terrain of Ceres, and surface temperature.

2. Dataset

Water ice in Juling crater has been detected during the High-Altitude Mapping Orbit (HAMO) phase (resolution ~400 m/px) and the Low Altitude Mapping Orbit (LAMO) phase (resolution ~100 m/px). We take into account an area on the northern rim which include an ice rich wall (Fig. 2) large enough to be spatially resolved even at the lowest resolution and that includes all the pixels of water ice signatures.

3. Method

The region of interest is in shadow. However, its signal can be detected using the light reflected by the crater. The radiance coming from the illuminated outer region is affecting the total signal collected in the shadowed region because of the Point Spread Function of the instrument (Fig. 1): the signal of the outer illuminated region is scattered in the adjacent pixels.
To account for this effect we model the signal collected (Eq. 1) as a weighted average of the signal from outer region (OR) (Eq. 2) and signal of the shadowed region (SR) (Eq. 3). The weights of these two different terrains are then retrieved by a best fitting procedure.
Moreover, the regolith of the shadowed ice-rich region (Eq. 2) is modeled by an areal mixture of water ice (WI) (optical constants by [6, 7, 8]), and Ceres' average terrain (CAT) with optical properties as defined by [9].

Eq. 1) $Refl_{average} = [Rad_{SR} * p_{SR} + Rad_{OR} * p_{OR}] / J$
where:
$Refl_{average}$ = average reflectance;
P_{SR} = cross section of the ice-rich shadowed region as a fraction of the total projected area of interest;
$p_{OR} = (1 - p_{SR})$ = cross section of the outer regions as a fraction of the total projected area of interest.

Eq. 2) $Rad_{OR} = J * r_{R\_OR}$
where:
Rad_{OR} = radiance of the outer regions;
J = solar irradiance;
r_{R_OR} = bidirectional reflectance [2] of Ceres' average terrain, with photometric parameters as defined by Ciarniello et al. (2016), and viewing geometry by

shape model analysis and spacecraft attitude at the moment of the observations;

Eq. 3) $Rad_{SR} = J * (r_{s\_CAT} <\mu_0> / \pi) /2 * [r_{s\_WI}\, p_{WI} + r_{s\_CAT}\, (1- p_{WI})]$

where:

Rad_{SR} = radiance of the shadowed ice-rich region;

r_{s_CAT} = bihemispherical reflectance [2] of Ceres' average terrain, it is used instead of the bidirectional reflectance because the secondary illumination hitting the shadow comes from all direction within ~π steradians;

$<\mu_0>$ is the average incidence angle cosine on the crater at the time of the observation, derived by shape model analysis;

the term $(r_{s\_CAT} <\mu_0> / \pi)$ represents the reflectance of a Lambertian surface, with Lambert albedo equal to r_{s_CAT} [2]; the factor 2 at denominator accounts for the fact that one half of the whole solid angle seen by the ice-rich wall is covered by the crater itself; higher orders of scattering are assumed as negligible.

r_{s_WI} = bihemispherical reflectance [2] of water ice;

p_{WI} = cross section of water ice as a fraction of the total projected area of the ice-rich shadowed region.

We model $Refl_{average}$ (Eq. 1) using a least square optimization algorithm that fitted the measured reflectance (similarly to [10]) to retrieve an unambiguously estimate of p_{SR} and p_{WI}.

Acknowledgments

The Visible and InfraRed mapping spectrometer (VIR) was funded and coordinated by the Italian Space Agency and built by SELEX ES, with the scientific leadership of the Institute for Space Astrophysics and Planetology, Italian National Institute for Astrophysics, Italy, and is operated by the Institute for Space Astrophysics and Planetology, Rome, Italy.

References

[1] De Sanctis M.C. et al., SSR 163, 2011.
[2] Hapke B., Cambridge Univ. Press., 2012.
[3] De Sanctis M.C. et al., Nature 528, 2015.
[4] Combe J.-Ph. et al., Science 353, 2016.
[5] Combe J.-Ph. et al., DPS-EPSC, 2016.
[6] Mastrapa R. M. et al., Icarus, 2008
[7] Mastrapa R. M. et al. , Astrophysical Journal, 2009
[8] Clark R. N. et al., Icarus, 218, 831, 2012.
[9] Ciarniello M. et al., A&A 2017
[10] Raponi A. et al., 2016, MNRAS 462.

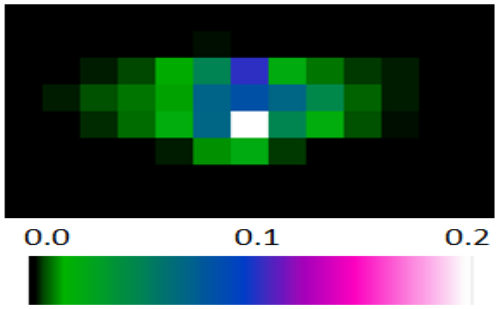

Figure 1. Point Sprad Function of VIR instrument as derived by a star observation.

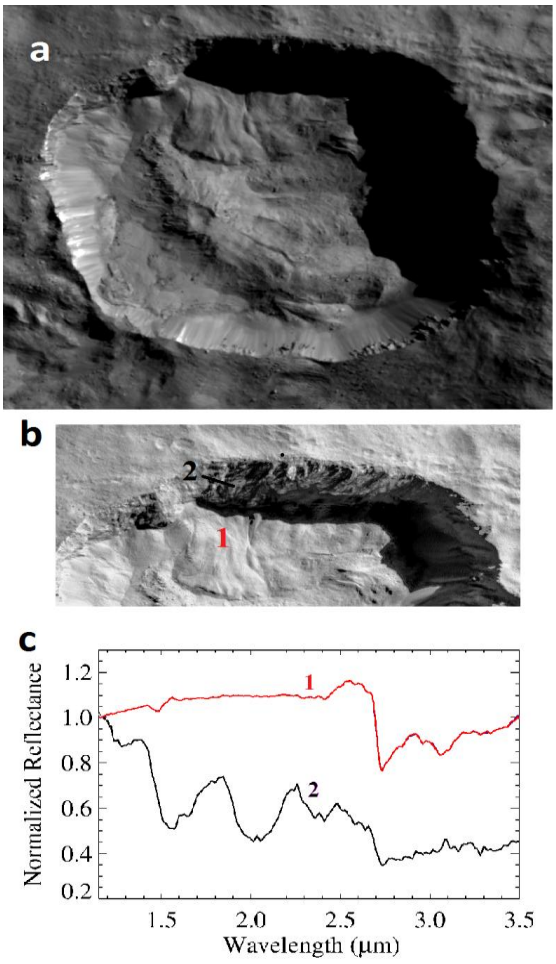

Figure2. Panel a) Juling crater: Framing camera mosaic. Panel b) Region of interest where shadows are enhanced in order to see the details. Panel c) typical spectra outside and inside the ice- rich shadowed.